Kinetic and Mechanistic Studies of Signal Peptidase I from *Escherichia coli*

Ross L. Stein,*,† Maria D. F. S. Barbosa,‡ and Robert Bruckner†

Departments of Chemical Enzymology and Antimicrobial Research, DuPont Pharmaceuticals Company, Experimental Station, E400/4460, Route 141 & Henry Clay Road, Wilmington, Delaware 19880

Received February 15, 2000; Revised Manuscript Received April 10, 2000

ABSTRACT: Signal peptidases of prokaryotic organisms reside in the outer leaflet of the cytoplasmic membrane and catalyze the hydrolytic cleavage of a specific peptide bond of membrane-imbedded preproteins to liberate mature proteins for secretion. In this manuscript, we report new and efficient peptide substrates for SPase and their use to explore features of this enzyme's reaction mechanism. The enzyme used in this study was recombinant SPase I of *Escherichia coli* that had been solubilized with Triton X-100 and purified to near homogeneity. Our new substrates are based on the fluorogenic peptide reported by Zhong and Benkovic [(1998) *Anal. Biochem. 255*, 66], Y^{NO2}FSASALA∼KIK^{Abz}-NH_2 (Y^{NO2}, 3-nitro-L-tyrosine; K^{Abz}, ϵ-(2-aminobenzoyl)-L-Lys; hydrolysis at A∼K). We found that when a signal peptide-like sequence is appended onto the N-terminus of this peptide to produce K_5-L_{10}-Y^{NO2}FSASALA∼KIK^{Abz}-NH_2, k_c/K_m increases from 85 to 2.5×10^6 M^{-1} s^{-1}. k_c/K_m decreases with increasing concentration of Triton X-100 micelles under the condition $[\text{Triton X-100}]_{micelle} > [S]_0 > [E]_0$. We explain this apparent inhibition with a model of surface dilution kinetics in which "empty" micelles compete with substrate-containing micelles for micelle-bound enzyme. Fusion of micelle-bound enzyme with a substrate-containing micelle leads to formation of productive E:S substrate complexes while fusion of micelle-bound enzyme with an "empty" micelle is nonproductive and inhibitory. The dependence of steady-state kinetic parameters for the SPase-catalyzed hydrolysis of K_5-L_{10}-Y^{NO2}FSASALA∼KIK^{Abz}-NH_2 on $[\text{Triton X-100}]_{micelle}$ supports this model. Product inhibition and solvent isotope effects were also investigated and could be interpreted in the context of this model.

Signal peptidases (SPases) play a key role in the protein secretary pathway of prokaryotic organisms (*1*−*6*). This pathway is highly conserved in bacteria and involves chaperonin-like molecules that transport the preprotein from the ribosome to the inner leaflet of the cytoplasmic membrane, where, in an ATP-dependent process, other protein elements of the pathway "thread" the preprotein through the membrane so that only the signal sequence of the preprotein is still bound to the membrane. In the final step of this process, signal peptidase hydrolytically cleaves the protein at the juncture of the signal sequence and mature protein and releases the latter for secretion.

SPases are membrane-bound proteins consisting of a single polypeptide chain that is anchored to the membrane by either one (gram-positive and some gram-negative bacteria) or two (gram-negative bacteria) N-terminal transmembrane sections (*7*). The active site of the enzyme is part of a C-terminal domain that is located on the extracellular side of the cytoplasmic membrane (*7*, *8*). It is thought that the active site may be partially immersed in the outer leaflet of the bilayer, allowing for more efficient cleavage of membrane-embedded signal sequences of preproteins (*9*).

The catalytic mechanism of SPase is unique and has been sorted out with a combination of mutagenesis and X-ray crystallographic studies (*7*, *8*, *10*). These experiments suggest that *Escherichia coli* SPase catalyzes amide bond hydrolysis by a mechanism involving nucleophilic attack by the hydroxyl of Ser^{90} with protolytic catalysis by the ϵ-amine of Lys^{145}. Sequence alignment of active site regions suggests that this mechanism is probably used by all signal peptidases (*7*). Comparison of the 18 known bacterial enzymes reveals two consensus sequences surrounding the two critical amino acid residues at the active site: −Ser-Gly-**Ser**-Met-Xaa-Pro-Thr-Leu− (Xaa = Met or Tyr) and −Xaa-Xaa-**Lys**-Arg-Xaa-Xaa-Gly-Pro-Gly-Asp− (Xaa = hydrophobic residues). This is despite an overall identity among the enzymes of only 8%.

One of the most interesting features of this enzyme's mechanism has emerged from studies of substrate specificity (*7*). These studies have revealed enormous disparities in catalytic efficiency between preprotein and peptide substrates. The best example of this is for the SPase-catalyzed hydrolysis of pro-OmpA-nuclease A and a nine amino acid peptide that spans the cleavage site of this protein. k_c/K_m is 2×10^6 M^{-1} s^{-1} for pro-OmpA-nuclease A and only 40 M^{-1} s^{-1} for the peptide (*11*).

Our goal in this study is to explore the disparity in SPase's catalytic efficiency toward preprotein and peptide substrates. We hypothesized that the origin of this disparity resides in the signal peptide sequence of the preprotein which serves two purposes in reactions of SPase: (1) a membrane anchor, to allow interaction between SPase and preprotein substrate; and (2) a determinant of the substrate specificity of SPase. To test this idea, we chose to use a surfactant micelle reaction

* To whom correspondence should be addressed. Phone: 302-695-1605. Fax: 302-695-8313. E-mail: Ross.L.Stein@dupontpharma.com.
† Department of Chemical Enzymology.
‡ Department of Antimicrobial Research.

10.1021/bi000352i CCC: $19.00
Published on Web 06/16/2000

system as our model. The enzyme we used was full-length, recombinant SPase I from *E. coli* that had been solubilized and embedded into Triton X-100 micelles. The new substrate we used, K_5-L_{10}-Y^{NO2}FSASALA∼KIK^{Abz}-NH_2,[1] was designed by combining elements of a signal peptide-like sequence (i.e., K_5-L_{10}-) with the core substrate reported by Zhong and Benkovic, Y^{NO2}FSASALA∼KIK^{Abz} (*12*).

We found that this signal peptide-extended peptide associates with micelles and is a remarkably efficient substrate for SPase. Our kinetic results further suggest that the increased reactivity of this substrate over simple peptide substrates is due to both an anchoring effect as well as specific interactions between SPase and the signal peptide-like portion of the substrate.

MATERIALS AND METHODS

General. Buffer salts, deuterium oxide, Triton X-100, and porcine pancreatic elastase were from Sigma Chemical Co. All curve-fitting was done with the software package GraFit (Erithacus Software, Staines, U.K.).

Peptides. All peptide substrates were purchased from New England Peptides (Fitchburg, MA). In all cases, purity was >98% as judged by HPLC analysis. Structure was confirmed by mass spectral analysis (MALDI-TOF DE; within 0.1% of exact molecular weight) and, in several cases, amino acid sequence analysis.

Cloning and Expression of Signal Peptidase. The *E. coli lepB* gene (*13*, *14*)was PCR amplified and inserted into the *BamHI* and *NdeI* sites of plasmid pET-26(+) (Novagen). The primers used for the amplification were as follows: forward primer, 5′-CGGGATCCATGGCGAATATGTTTGCC-3′; reverse primer, 5′-GGAATTCCATATGCGTGAACGAAGATGGCTATTA-3′. Chromosomal DNA from *E. coli* K12 MG1655 was prepared with a Qiamp tissue kit (Qiagen) and utilized as template for the PCR reaction. The sequence of the cloned gene was analyzed with the GCG Package (*15*). For the expression of SPase, 3 L of LB containing 15 μg/mL kanamycin and 34 μg/mL chloramphenicol was inoculated with a $^1/_{50}$ dilution of an overnight culture of *lepB*/pET26b/BL21pLysS. Cells were grown at 37 °C until an OD_{595} of 0.8 was reached (∼3 h) at which time 1 μM IPTG was added to induce SPase. The IPTG-treated cell suspension was shaken for an additional 4 h. Cells were then harvested by centrifugation at 10 000 rpm for 30 min and the resultant cell pellets resuspended in 80 mL of 50 mM Tris-HCl, pH 8.0, containing 10% sucrose (w/v) and protease inhibitors (CalBiochem Protease Inhibitor Cocktail Set 2; as per manufacturer's instructions). This suspension of cells was frozen in liquid nitrogen and stored at −80 °C.

Signal Peptidase Purification. A cell suspension was thawed at 37 °C, treated with DNase I (10 000 units; Gibco BRL) and $MgCl_2$ (6 mM), and allowed to incubate at room temperature for 60 min. After this incubation, the suspension was centrifuged for 90 min at 19 000 rpm, the supernatant removed, and the pellets resuspended in 70 mL of 20 mM Tris-HCl, pH 8.0, buffer containing 1 mM EDTA and protease inhibitors (buffer A). The suspension was sonicated in a Branson Sonifier 450 (50% cycle, power setting 8) four times for 30 s with cooling between bursts. The sonicated suspension was centrifuged at 200 000*g* for 60 min. Pellets were collected and resuspended in 36 mL of buffer A and sonnicated three times for 30 s. A 4 mL volume of 10% Triton X-100 was added, and the mixture was stirred gently overnight at 4 °C and then centrifuged at 200 000*g* for 90 min. At a flow rate of 0.5 mL/min, 50 mL of the supernatant was loaded onto a column of BioRad Macro-Prep DEAE (6.0 × 2.5 cm; 30 mL) that had been equilibrated with buffer A plus 1.0% Triton X-100. The column was washed with buffer A plus Triton X-100. Flow-through and wash fractions were collected. Fractions that contained SPase were identified by enzymatic acitivy toward our synthetic substrate (see below for details of assay). These fractions were pooled (53 mL) and diluted by the addition of 53 mL of 20 mM Tris-HCL pH 8.5 containing 1 mM EDTA and 1.0% Triton X-100 (buffer B) and 4 mL of 1 M Tris-HCl pH 8.5. At a flow rate of 1 mL/min, this SPase-containing solution was loaded onto a 10 mL (two 5 mL cartridges in tandem) BioRad High Q column that had been equilibrated in buffer B. The column was washed with 40 mL buffer B and subsequently eluted with a 200 mL linear gradient from 0 to 200 mM NaCl in buffer B. SPase-containing fractions were pooled (30 mL) and frozen in aliquots. Protein determination of this pooled fraction was with a BioRad Dc Protein Assay Kit using BSA in 1% Triton X-100 as a standard.

Chromatographic and Mass Spectral Analysis of the Hydrolysis of K_5-L_{10}-Y^{NO2}FSASALA∼KIK^{Abz}-NH_2 by SPase. A 12 μL volume of a 10 mM stock solution of K_5-L_{10}-Y^{NO2}-FSASALA∼KIK^{Abz}-NH_2 in DMSO and 1.7 μL of a 28 μM stock solution SPase were added to 6 mL of standard reaction buffer (50 mM Tris/HCl, 1% Triton X-100, pH 8.1) and incubated at 37 °C ($[E]_{final}$ = 8.6 nM; $[S]_{final}$ = 20 μM). At predetermined times, a 450 μL aliquot was removed from the reaction solution and filtered through 10 kDa cutoff ultrafiltration unit (Amicon). A 50 μL volume of the resulting filtrate was subjected to reverse phase HPLC analysis (NovaPak C18 column; eluted with a linear gradient from 0 to 90% AcCN/0.1% TFA over 25 min) with fluorescence detection (λ_{ex} = 340 nm; λ_{em} = 412 nm). A single fluorescent peak eluted, and the material was subjected to mass spectral analysis.

Kinetic Methods: Hydrolysis of K_5-L_{10}-Y^{NO2}FSASALA∼KIK^{Abz}-NH_2. This assay relies on the ability of the nitrophenol of Y^{NO2} to internally quench the fluorescence of the 2-aminobenzoyl group of K^{Abz}. When the peptide is hydrolyzed, the internal quenching is released and an increase in fluorescence intensity at 412 nm is observed. Similar assays have been described for other proteases, including signal peptidase (*12*).

In a typical kinetic run, 1−10 μL of a solution of K_5-L_{10}-Y^{NO2}FSASALA∼KIK^{Abz}-NH_2 in DMSO was added to 2.00 mL of assay buffer (50 mM Tris/HCl, 1% Triton X-100, pH 8.1) in a 3 mL fluorescence cuvette, and the cuvette was placed in the jacketed cell holder of a Perkin-Elmer LS-50B fluorometer. Reaction temperature was maintained at 37.0 ± 0.1 °C by a circulating water bath. After the reaction solution had reached thermal equilibrium (∼5 min), 1−5 μL of stock SPase was added to the cuvette. Reaction progress was monitored by the increase in fluorescence intensity at 412 nm (λ_{ex} = 340 nm) that accompanies cleavage of the

[1] Abbreviations: AMC, aminomethylcoumarin; Y^{NO2}, 3-nitro-L-tyrosine; K^{Abz}, ϵ-(2-aminobenzoyl)-L-Lys; hydrolysis at A∼K.; preMBP, protein precursor of maltose binding protein; OmpA, outer membrane protein A.

peptide substrate. For each kinetic, run 100−3000 data points, corresponding to {time, FI} pairs, were collected by a PC interfaced to the fluorometer.

Kinetic runs, for both full progress curve analyses and initial velocity measurements, were monitored until >98% of the substrate had been hydrolyzed and we could establish an accurate estimate of the reaction end point. For full progress curve analysis, this is necessary for least-squares fitting to the integrated Michaelis−Menten equation. For initial velocity measurements, an accurate estimate of the reaction endpoint allows us to convert the units of the observed velocities from FI/s to nM/s using the expression

$$v_{\mathrm{nM/s}} = \frac{v_{\mathrm{FI/s}}}{(\mathrm{FI}_{t=\infty} - \mathrm{FI}_{t=0})/[S]_0} \quad (1)$$

where $v_{\mathrm{nM/s}}$ is the reaction velocity in units of nM/s, $v_{\mathrm{FI/s}}$ is the reaction velocity in units of fluorescence intensity/s, $\mathrm{FI}_{t=\infty}$ is the fluorescence intensity at infinite time (i.e., the end point reading), $\mathrm{FI}_{t=0}$ is the fluorescence intensity at time zero, and $[S]_0$ is the initial substrate concentration in nM units.

Kinetic Methods: Hydrolysis of $Y^{NO2}FSASALA\sim KIK^{Abz}$-$NH_2$. Kinetic analysis of the SPase-catalyzed hydrolysis of $Y^{NO2}FSASALA\sim KIK^{Abz}$-$NH_2$ was similar to that for hydrolysis of K_5-L_{10}-$Y^{NO2}FSASALA\sim KIK^{Abz}$-$NH_2$ except in the determination of the end point (i.e., $\mathrm{FI}_{t=\infty}$) for calculation of reaction velocity. These reactions were so slow as to prohibit monitoring the reaction to completion. To determine the end point, a 20 μL aliquot of a 0.1 mM solution of porcine pancreatic elastase was added to completely hydrolyze the substrate (probably at the Ala−Leu bond). Addition of the aliquot of elastase was done after we had accumulated sufficient data to allow accurate calculation of an initial velocity.

Kinetic Methods: Hydrolysis of K_5-L_{10}-$YFSASALA\sim KIK^{Abz}$-NH_2. The fluorescence of K^{Abz} is not internally quenched in this peptide, but rather the fluorescence intensity is enhanced when the peptide inserts into the Triton X-100 micelle. Thus, hydrolysis of this peptide by SPase can be followed by the decrease in fluorescence intensity at 412 nm ($\lambda_{ex} = 350$ nm) that occurs as the Ala−Lys bond is cleaved and the product KIK^{Abz}-NH_2 diffuses away from the micelle into bulk aqueous solvent.

Kinetic Methods: Hydrolysis of K_5-L_{10}-$YFSASALA\sim AMC$. Hydrolysis of this peptide by SPase liberates the intensely fluorescent AMC group which was monitored at $\lambda_{ex} = 380$ nm and $\lambda_{em} = 438$ nm.

Micelle Concentration for Triton X-100. The concentration of Triton X-100 micelles was calculated according to $[\text{Triton X-100}]_{\mathrm{micelle}} = ([\text{Triton X-100}] - \mathrm{CMC})/\text{aggregation number}$, where CMC = 0.3 mM and aggregation number = 140 (*29*, *30*). For nonionic detergents such Triton X-100, CMC and aggregation number are largely insensitive to temperature, ionic strength, and pH in the general range used in the experiments.

Solvent Deuterium Isotope Effects: Preparation of Buffers. The H_2O buffer was prepared by diluting 5 mL of a 10% solution of Triton X-100 in H_2O and 2.5 mL of a 1.0 M Tris/HCl, pH 8.0, stock solution to a final volume of 50.0 mL with distilled water to provide a solution with a pH of 8.1. Similarly, the D_2O buffer was prepared by diluting 5 mL of a 10% solution of Triton X-100 in H_2O and 2.5 mL of a 1.0 M Tris/HCl, pH 8.0, stock solution to a final volume of 50.0 mL with D_2O (99.9% D) to provide a solution with a pH metering reading of 8.2 and final % D of 85%.

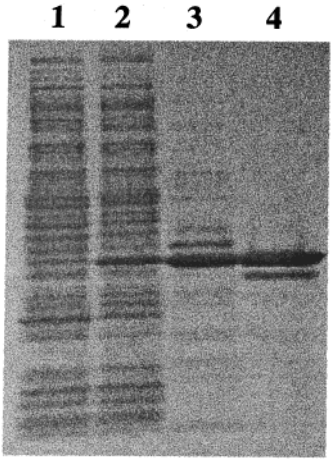

FIGURE 1: Purification of signal peptidase I from *E. coli*: lane 1, soluble fraction of lysed cells; lane 2, Triton X-100 extract of pellet of lysed cells; lane 3, active fraction of an isocratic elution from DEAE-Sepharose; lane 4, active fraction of a gradient elution from High Q. Activity was measured using $Y^{NO2}FSASALA\sim KIK^{Abz}$-$NH_2$ ([S] = 10 μM, 50 mM Tris/HCl, 1% Triton X-100, pH 8.1, 37 °C).

RESULTS

Purification of Signal Peptidase I from E. coli. Figure 1 summarizes the purification of our recombinant SPase. The active fraction that elutes from the High Q column is a near homogeneous preparation with only a minor low molecular weight contaminant of autolysis product (below). This fraction provided our final, working stock solution of SPase of 1 mg/mL (~28 μM) in 50 mM Tris/HCl, 1% Triton X-100, pH 8.1. The concentration of enzyme was based on protein determination.

Signal Peptidase-Catalyzed Hydrolysis of the Minimal Substrate, $Y^{NO2}FSASALA\sim KIK^{Abz}$-$NH_2$. Recently, Zhong and Benkovic reported a continuous, fluorometric assay based on the hydrolysis of $Y^{NO2}FSASALA\sim KIK^{Abz}$ (*12*). We prepared the primary amide of this peptide, $Y^{NO2}FSASALA\sim KIK^{Abz}$-$NH_2$, and found that it too was hydrolyzed by SPase. Initial velocities for hydrolysis of $Y^{NO2}FSASALA\sim KIK^{Abz}$-$NH_2$ by SPase are linearly dependent on both enzyme concentration (0.1−2 μM) and substrate concentration (1−10 μM). The slope of the dependence of initial velocity on substrate concentration yielded a value of k_c/K_m of 85 ± 18 $M^{-1}\,s^{-1}$ (see Table 1) that is identical to that found by Zhong and Benkovic. Initial velocities for the hydrolysis of $Y^{NO2}FSASALA\sim KIK^{Abz}$-$NH_2$ by SPase is independent of Triton X-100 concentration over the range 0.005%−2% (0.085−34 mM; CMC = 0.3 mM).

Association of K_5-L_{10}-$Y^{NO2}FSASALA\sim KIK^{Abz}$-$NH_2$ with Triton X-100 Micelles. To produce a peptide substrate of greater catalytic efficiency toward SPase, we reasoned that if we could design substrates that would associate with surfactant micelles, these substrates would more readily form productive complexes with micelle-embedded SPase. To this end, we appended a signal peptide-like sequence to the N-terminus of the minimal substrate, $Y^{NO2}FSASALA\sim KIK^{Abz}$-$NH_2$, to produce K_5-L_{10}-$Y^{NO2}FSASALA\sim KIK^{Abz}$-

Table 1: Steady-State Kinetic Parameters for Catalysis by Signal Peptidase[a]

substrate	$(k_c/K_m)_{obs}$ (M^{-1} s^{-1})	$k_{c,obs}$ (s^{-1})	$K_{m,obs}$ (μM)
Y^{NO2}FSASALA~KIK^{Abz}-NH_2[b]	85	(10^{-2}−10^{-3})	(10^2−10^3)
K_5-L_{10}-Y^{NO2}FSASALA~KIK^{Abz}-NH_2[c]	2,500,000	1.5	0.6

[a] Reaction conditions: 50 mM Tris/HCl, 0.03% ([Triton X-100]$_{micelle}$ = 1.3 μM), pH 8.1, 37 °C. [b] $(k_c/K_m)_{obs}$ was determined from the slope of the linear dependence of initial velocity on substrate concentration ($1 < [S]_0 < 10$ μM) at [SPase] = 0.3 μM. Replicate determinations of this value over several months indicate a relative standard deviation of 20%. Values of $k_{c,obs}$ and $K_{m,obs}$ are ranges taken from the literature (*16*, *17*). [c] Values of steady-state kinetic parameters for this substrate were determined by progress curve analysis as illustrated in Figure 3 and described in the text. Replicate determinations indicate relative standard deviations for these parameters of no greater than 10%.

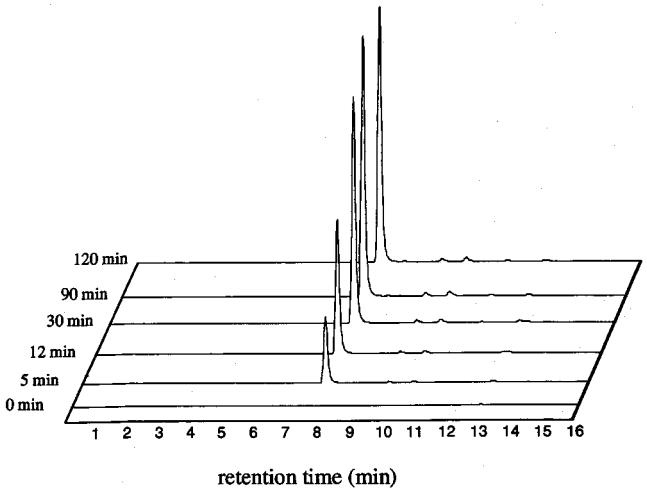

FIGURE 2: Hydrolysis of K_5-L_{10}-Y^{NO2}FSASALA~KIK^{Abz}-NH_2 by SPase. The chromatographic tracings correspond to fluorescence detection (λ_{ex} = 340 nm; λ_{em} = 412 nm) of 20 μL aliquots of the filtrate (10 kDa cutoff) of an SPase reaction solution (see Material and Methods). A single low molecular weight reaction product is observed with a retention time of 8.2 min. Reaction conditions: [S] = 20 μM, [E] = 8.6 nM; 50 mM Tris/HCl, 1% Triton X-100, pH 8.1, 37 °C.

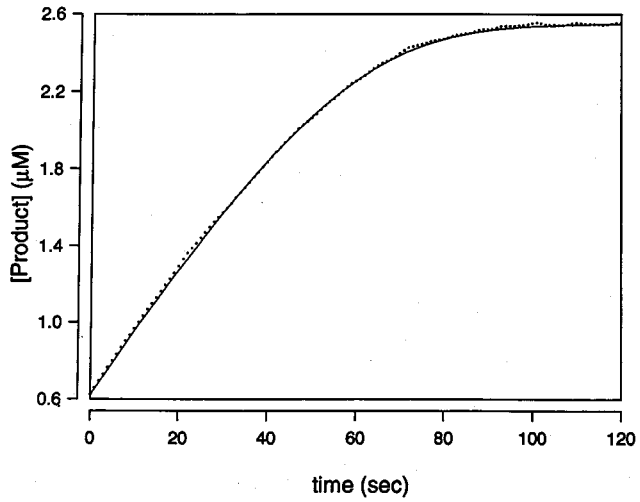

FIGURE 3: Reaction progress curve for the SPase-catalyzed hydrolysis K_5-L_{10}-Y^{NO2}FSASALA~KIK^{Abz}-NH_2. Fluorescence intensities were converted to product concentration, using the expression $[P]_t = [S]_0\{1 - (FI_{t=\infty} - FI_t)/(FI_{t=\infty} - FI_0)\}$, and plotted vs time. The solid line through the data was drawn using the best-fit parameters obtained from fitting the data fit to integrated Michaelis−Menten equation, V_{max} = 43.1 ± 0.2 nM/s and K_m = 0.51 ± 0.01 μM. Reaction conditions: [S] = 2.6 μM, [E] = 35 nM; 50 mM Tris/HCl, 1.86 μM Triton X-100 micelles, pH 8.1, 37 °C.

NH_2. Our first experiments were to determine if K_5-L_{10}-Y^{NO2}FSASALA~KIK^{Abz}-NH_2 and structurally related peptides, such as K_5-L_{10}-YFSASALA~KIK^{Abz}-NH_2, in fact, associate with Triton X-100 micelles. Two methods were used to determine this.

In the first, we passed a 2 μM solution of K_5-L_{10}-YFSASALA~KIK^{Abz}-NH_2 in 50 mM Tris/HCl, pH 8.1, 1% Triton X-100 through a 10 kDa cutoff filter and determined that there was no fluorescence in the micelle-free filtrate. We conclude from this experiment that K_5-L_{10}-YFSASALA~KIK^{Abz}-NH_2 is associated with the Triton micelle.

In the second method, we determined and compared fluorescence emmision spectra for K_5-L_{10}-YFSASALA~KIK^{Abz}-NH_2 and KIK^{Abz}-NH_2 (2 μM solutions in 50 mM Tris/HCl, pH 8.1, 1% Triton X-100; λ_{ex} = 340 nm) Two observations are important: (i) The fluorescence intensity of the longer peptide is 3-fold greater than the intensity of shorter peptide. (ii) $\lambda_{em,max}$ is 405 nm for the longer peptide while $\lambda_{em,max}$ is 409 nm for the shorter peptide. As above, these observations support micelle-associated K_5-L_{10}-YFSASALA~KIK^{Abz}-NH_2.

Signal Peptidase-Catalyzed Hydrolysis of K_5-L_{10}-Y^{NO2}-FSASALA~KIK^{Abz}-NH_2. Having established that this peptide is associated with Triton X-100 micelles, we next determined if it is a substrate for SPase. As we anticipated, this peptide was found to be an efficient substrate for SPase.

Figure 2 summarizes a chromatographic analysis of the hydrolysis of K_5-L_{10}-Y^{NO2}FSASALA~KIK^{Abz}-NH_2 by SPase and illustrates that only a single C-terminal hydrolysis product is produced, even upon prolonged incubation of enzyme and substrate. Mass spectral analysis identified this product as KIK^{Abz}-NH_2. The high efficiency of hydrolysis is indicated by the observation of nearly complete hydrolysis of 20 μM substrate in 30 min by only 9 nM enzyme.

Steady-state kinetic parameters for the SPase-catalyzed hydrolysis of K_5-L_{10}-Y^{NO2}FSASALA~KIK^{Abz}-NH_2 were determined using the continuous assay described in the Materials and Methods section. Figure 3 illustrates one of our methods of kinetic analysis for the SPase-catalyzed hydrolysis of K_5-L_{10}-Y^{NO2}FSASALA~KIK^{Abz}-NH_2. Here, we fit a full reaction progress curve to the integrated Michaelis−Menten equation to arrive at values of V_{max} and K_m. This method of analysis proved useful for this system because of the relatively low sensitivity of the assay; that is, only a 2−4-fold increase in fluorescence intensity is observed upon complete hydrolysis of micelle-bound K_5-L_{10}-Y^{NO2}-FSASALA~KIK^{Abz}-NH_2.

Table 1 summarizes a comparison of steady-state kinetic parameters for the SPase-catalyzed hydrolysis of Y^{NO2}FSASALA~KIK^{Abz}-NH_2 and K_5-L_{10}-Y^{NO2}FSASALA~KIK^{Abz}-NH_2 at limiting micelle concentration of Triton X-100 (see below for micelle concentration dependence of SPase catalysis).

Product Inhibition of Signal Peptidase. As part of our validation of the progress curve method (see above), we

collected and analyzed full reaction progress curves at initial substrate concentrations ranging from 1.25 to 40 μM (50 mM Tris/HCl, 1% Triton X-100, pH 8.1, 37 °C). In the absence of kinetic complexity, the steady-state kinetic parameters that are obtained from this analysis should be independent of the initial concentration of substrate, $[S]_0$. Contrary to this simple expectation, we observed a marked dependence of these parameters on $[S]_0$. We found that as we increased $[S]_0$ from 1.25 to 40 μM, the calculated value of K_m increased linearly from 2 to 20 μM while the calculated value of k_c/K_m decreased from 300 000 to 80 000 M^{-1} s^{-1} in accordance with a simple binding isotherm with $IC_{50} \sim 10$ μM (data not shown). This sort of behavior is diagnostic of competitive product inhibition; that is, for enzymes that are susceptible to product inhibition, high initial substrate concentrations ultimately produce high concentrations of product which results in an increase in observed values of K_m and a decrease in observed values of k_c/K_m.

Two methods were used to provide a quantitative analysis of this phenomena: (i) dependence of $k_{terminal}$ on $[S]_0$, where $k_{terminal}$ is the first-order rate constant obtained from fitting terminal portions of reaction progress curves to a simple first order rate law; (ii) inhibition by exogeneously added product, K_5-L_{10}-Y^{NO2}FSASALA.

The first method is based on fact that, at substrate concentrations below K_m, reaction progress curves have a first-order dependence on substrate concentration with pseudo-first-order rate consant, $k_{obs} = (k_c/K_m)[E]_0$. Now, if one conducts a kinetic experiment in which $[S]_0$ is greater than K_m, the first-order region of the progress curve will eventually be reached but only after much of the substrate has been consumed. Fitting these terminal regions of reaction progress curves to a first-order rate law provides values of a pseudo-first-order rate constant that we designate $k_{terminal}$. In the absence of kinetic complexity, $k_{terminal} = (k_c/K_m)[E]_0$. If the enzyme is susceptible to competitive product inhibition, the product which has accumulated will inhibit the enzyme. This will be manifested kinetically as a $[S]_0$-dependent decrease in $k_{terminal}$ which now equals $(k_c/K_m)[E]_0/(1 + [S]_0/K_{i,app})$. In this equation, $[S]_0 \sim [P]_\infty$ and $K_{i,app}$ is the dissociation constant of the enzyme:product complex.

Figure 4 summarizes results of experiments using both of these methods. Both data sets describe simple binding isotherms with $K_{i,app}$ values of around 10 μM. Note that this value agrees with the qualitative analysis described above for full progress curve analysis where we noted a $[S]_0$-dependent decrease in k_c/K_m.

Dependence of Signal Peptidase Catalysis on Triton X-100 Concentration. Figure 5 shows the dependence of k_c/K_m on Triton X-100 concentration for the SPase-catalyzed hydrolysis of K_5-L_{10}-Y^{NO2}FSASALA~KIK^{Abz}-NH_2. At concentrations of Triton X-100 that are above its CMC of 0.3 mM, the data are well behaved and suggest an apparent inhibition by this surfactant with a $(k_c/K_m)_{obs,limit}$ of 2.2×10^6 M^{-1} s^{-1} being titrated with $K_{i,app}$ equal to 3.1 mM. Below the CMC, there is more scatter and less reproducibility in the data.

A more detailed examination of the dependence of SPase catalysis on Triton X-100 concentration is provided in Figure 6, where we plot observed values of steady-state kinetic parameters as a function of the concentration Triton X-100 micelles. In panel A, we see little dependence of $k_{c,obs}$ on $[\text{Triton X-100}]_{micelle}$. The small, inverse dependence is not

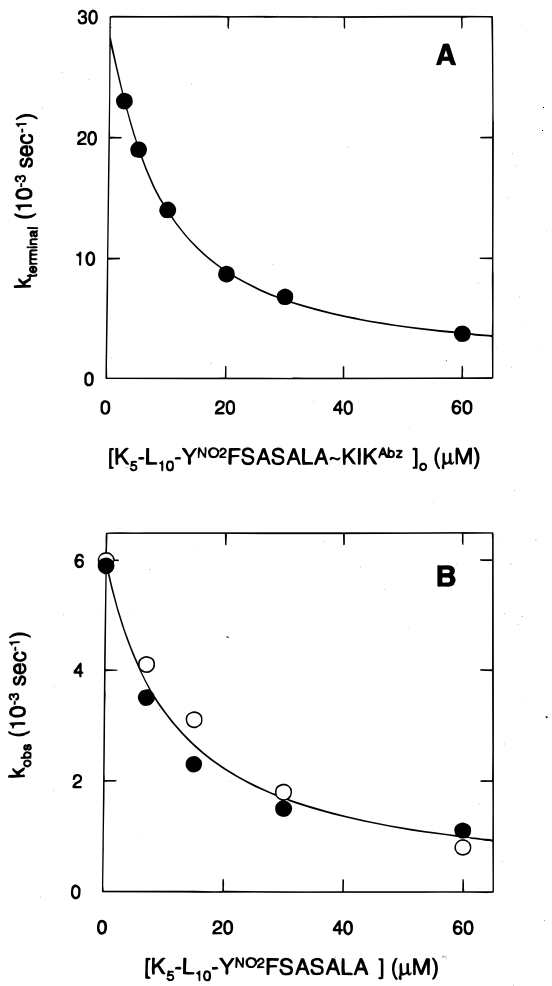

FIGURE 4: Product inhibition of SPase. Panel A: Dependence of $k_{terminal}$ on initial substrate concentration for the SPase-catalyzed hydrolysis of K_5-L_{10}-Y^{NO2}FSASALA~KIK^{Abz}-NH_2, where $k_{terminal}$ is the first-order rate constant obtained from fitting the terminal portion of reaction progress curves to a simple first-order rate law. The solid line was drawn using the equation for a simple binding isotherm and the best-fit parameters, $k_{terminal,limit} = (29 \pm 1) \times 10^{-3}$ s^{-1} and $K_{i,app} = 9.3 \pm 0.9$ μM. Reaction conditions: [E] = 140 nM; 50 mM Tris/HCl, 1% Triton X-100, pH 8.1, 37 °C. Panel B: Dependence of k_{obs} on the concentration of K_5-L_{10}-Y^{NO2}FSASALA, where k_{obs} is the first-order rate constant obtained from fitting reaction progress curves recorded at low substrate concentration ([K_5-L_{10}-Y^{NO2}FSASALA~KIK^{Abz}-NH_2] = 0.5 μM) to a simple first-order rate law. The filled and open circles reflect data from two independent experiments. The solid line was drawn using the equation for a simple binding isotherm and the best-fit parameters, $k_{obs,limit} = (6.0 \pm 0.3) \times 10^{-3}$ s^{-1} and $K_{i,app} = 12 \pm 1$ μM. Reaction conditions: [E] = 28 nM; 50 mM Tris/HCl, 1% Triton X-100, pH 8.1, 37 °C.

reproducible and we believe not mechanistically significant. In contrast, the dependence of $(k_c/K_m)_{obs}$ on $[\text{Triton X-100}]_{micelle}$, as illustrated in panel B, is described by an inhibition titration curve with a $K_{i,app}$ value of 15 ± 1 μM and a limiting value of $(k_c/K_m)_{obs}$ of $(2.5 \pm 0.8) \times 10^6$ M^{-1} s^{-1}. Finally, panel C shows the dependence of $K_{m,obs}$ on $[\text{Triton X-100}]_{micelle}$ which is linear with a *y*-intercept of 0.61 ± 0.08 μM and a slope of $(2.7 \pm 0.2) \times 10^{-2}$.

These data as well as those of Figure 5 are consistent with the mechanism of surfactant-dependent catalysis that is developed below.

Solvent Isotope Effects for Catalysis by Signal Peptidase. For the SPase-catalyzed hydrolysis of K_5-L_{10}-Y^{NO2}-

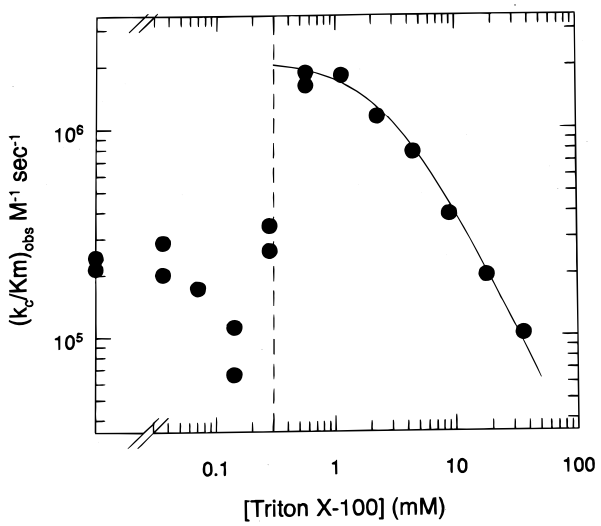

FIGURE 5: Dependence of $(k_c/K_m)_{obs}$ for the SPase-catalyzed hydrolysis K_5-L_{10}-Y^{NO2}FSASALA∼KIK^{Abz}-NH_2 on Triton X-100 concentration. The dashed vertical line marks the CMC of Triton X-100 at 0.3 mM. The solid line was drawn using the equation for a simple binding isotherm and the best-fit parameters for the data recorded at [Triton X-100] > 0.3 mM, $(k_c/K_m)_{obs,limit} = 2.15 \pm 0.03$ μM^{-1} s^{-1}, and $K_{i,app} = 3.1 \pm 0.2$ mM. Reaction conditions: [S] = 2 μM, [E] = 35 nM; 50 mM Tris/HCl, pH 8.1, 37 °C.

FSASALA∼KIK^{Abz}-NH_2, values of $(k_c/K_m)_{obs}$ were determined in H_2O and D_2O buffers to be 194 ± 12 and 179 ± 3 mM^{-1} s^{-1}, respectively (four kinetic runs in each buffer). The ratio of rate constants is 1.08 ± 0.06. Since the D_2O buffer has $n_{D_2O} = 0.85$ (see Materials and Methods), the calculated ratio needs to be corrected according to a rearrangement of the Gross−Butler equation (*25*; see eq 9) to generate the true solvent isotope effect (i.e, $k_{n=0}/k_{n=1}$). This corrected value is 1.10 ± 0.07.

In contrast to this value of unity, the solvent isotope effects on $k_{c,obs}$ and $(k_c/K_m)_{obs}$ for the SPase-catalyzed hydrolysis of K_5-L_{10}-YFSASALA∼AMC are 2.22 ± 0.11 and 2.49 ± 0.13, respectively. These values were calculated from the results of the proton inventory study as the reciprocals of the fractionation factors (see below and Figure 7).

To aid in the interpretation of the solvent isotope effect results, we determined proton inventories (*25*) of $k_{c,obs}$ and $(k_c/K_m)_{obs}$ for the SPase-catalyzed hydrolysis of K_5-L_{10}-YFSASALA∼AMC (see Figure 7). In these experiments, we determined the dependencies of $k_{c,obs}$ and $(k_c/K_m)_{obs}$ on mole fraction solvent deuterium (see Table 2). Both of these dependencies were found to be linear.

Autolysis of Signal Peptidase. As Figure 8 illustrates, SPase (MW = 35 kDa) autolyzes to a smaller species (*19*) (MW = 32 kDa) that retains hydrolytic activity against the minimal substrate, Y^{NO2}FSASALA∼KIK^{Abz}-NH_2, but loses its ability to hydrolyze K_5-L_{10}-Y^{NO2}FSASALA∼KIK^{Abz}-NH_2. This autolytic reaction appears to be bimolecular since the dependence of reciprocal SPase concentration on time is linear. The slope of this line is equal to the inverse of the second-order rate constant for autolysis, 5 M^{-1} s^{-1}.

N-terminal sequence analysis of the autolysis product indicates that the first 40 residues have been removed to generate the species, Δ1−40 SPase. This correcsponds the removal of H1 (*7*), the first hydrophobic, transmembrane domain of SPase that extends from residues 1 to 22, and about half of P2, a cytoplasmic domain that extends from residues 23 to 62. The autolysis product, Δ1−40 SPase, has been observed before (*19*).

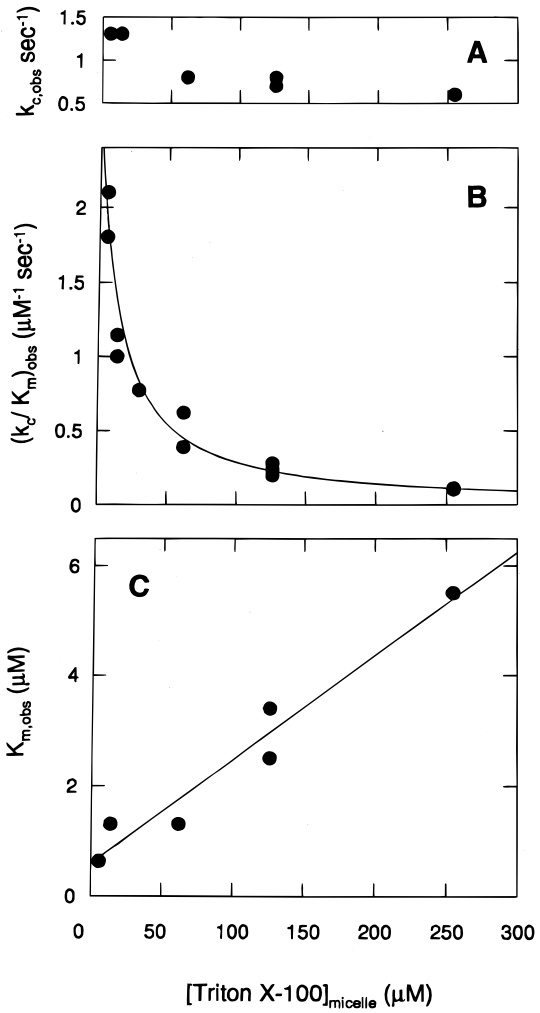

FIGURE 6: Dependence of observed steady-state kinetic parameters for SPase catalysis on the concentration of Triton X-100 micelles. As a function of Triton X-100 concentration, full reaction progress curves were recorded at [K_5-L_{10}-Y^{NO2}FSASALA∼KIK^{Abz}-NH_2] = 2.6 μM and [SPase] = 35 nM and fit to the integrated Michaelis−Menten equation. In panels A−C are plotted the best fit values of $k_{c,obs}$, $K_{m,obs}$, and $(k_c/K_m)_{obs}$, respectively, as a function of the concentration Triton X-100 micelles calculated according to [Triton X-100]$_{micelle}$ = ([Triton X-100] − CMC)/aggregation number, where CMC = 0.3 mM and aggregation number = 140. Reaction conditions: 50 mM Tris/HCl, pH 8.1, 37 °C.

DISCUSSION

Substrate Design for Signal Peptidase. The internally quenched, fluorogenic peptide Y^{NO2}FSASALA∼KIK^{Abz} was recently reported by Zhong and Benkovic to be a substrate for *E. coli* SPase with a k_c/K_m value of 70 M^{-1} s^{-1} (*12*). The sequence of this substrate was based on earlier work by Dev and co-workers who, in 1990, reported the first peptide substrates for SPase (*16*). The substrates that were developed by Dev were all based on the cleavage site in preMBP and had K_m values around 2 mM and k_c values that ranged from 6×10^{-6} to 3×10^{-2} s^{-1}. The most rapidly cleaved peptide (FSASALA∼KI; $k_c = 3 \times 10^{-2}$ s^{-1}, $K_m = 0.8$ mM, and $k_c/K_m = 38$ M^{-1} s^{-1}) became the model for the Zhong and Benkovic peptide. Another preMBP-based peptide was reported by Knight and co-workers and has the sequence

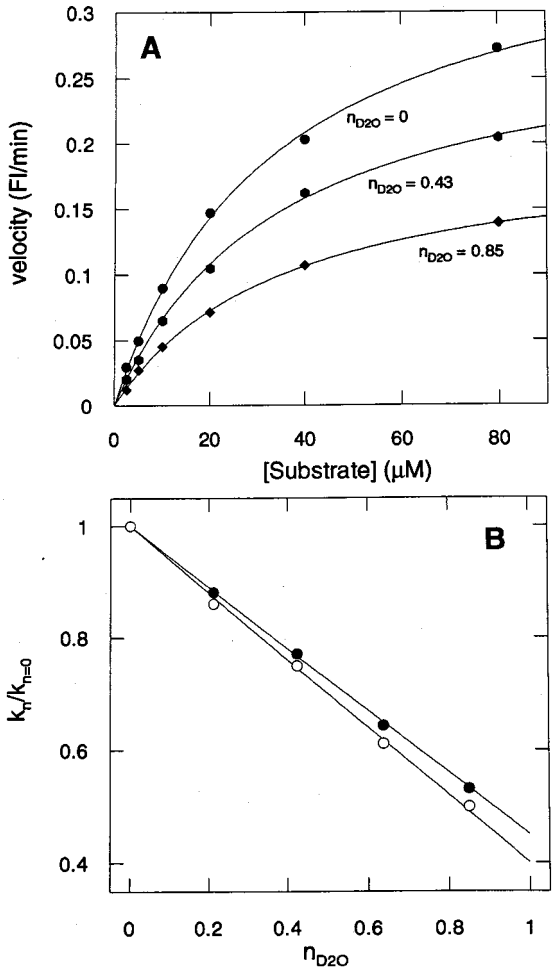

FIGURE 7: Proton inventory for SPase-catalyzed hydrolysis of K_5-L_{10}-YFSASALA∼AMC. Panel A depicts the dependence of steady-state velocity on substrate concentration at three mole fractions of solvent deuterium. Solid lines were drawn using the best-fit values according to the Michaelis−Menten equation (see Table 2). Panel B: Values of $k_{c,obs}$ (solid circles) and $(k_c/K_m)_{obs}$ (open circles) were plotted vs the mole fraction solvent deuterium at which they were determined (see Table 2). The solid lines were drawn using eq 9 and the best fit parameters: $\phi^T = 0.451 \pm 0.023$ and $\phi^T = 0.402 \pm 0.021$ for $k_{c,obs}$ and $(k_c/K_m)_{obs}$, respectively. For clarity in panel A, only three of the five Michaelis−Menten plots that were used in the construction of the proton inventory are shown. Reaction conditions: [E] = 70 nM; 50 mM Tris/HCl, 1% Triton X-100, pH 8.1, 37 °C.

Table 2: Proton Inventory Data for the Signal Peptidase-Catalyzed Hydrolysis of K_5-L_{10}-YFSASALA∼AMC[a,b]

n_{D_2O}	$k_{c,obs}$ (10^{-4} s^{-1})	$K_{m,obs}$ (μM)	$(k_c/K_m)_{obs}$ (M^{-1} s^{-1})
0.00	5.28 ± 0.15	32.8 ± 2.0	16.1 ± 0.6
0.21	4.67 ± 0.14	33.9 ± 2.1	13.7 ± 0.5
0.43	4.07 ± 0.13	34.0 ± 2.0	13.0 ± 0.5
0.64	3.40 ± 0.13	34.7 ± 2.2	9.4 ± 0.4
0.85	2.80 ± 0.08	35.4 ± 1.8	7.9 ± 0.2

[a] Reaction conditions: 50 mM Tris/HCl, 0.03% ($[Triton X-100]_{micelle}$ = 1.3 μM), pH 8.1 and pD equivalent, 37 °C. [b] Steady-state rate constants were determined from fitting the substrate concentration dependence of steady-state velocity to the Michaelis−Menten equation at each of the five mole fractions of solvent deuterium (see Figure 7A for examples). The error estimates are from the fitting procedure.

Ac-WSASALA∼KI-AMC (*17*). In the assay developed using this substrate, SPase-catalyzed hydrolysis of parent peptide liberates KI-AMC which is rapidly hydrolyzed by exogenously added aminopeptidase to liberate free AMC. The

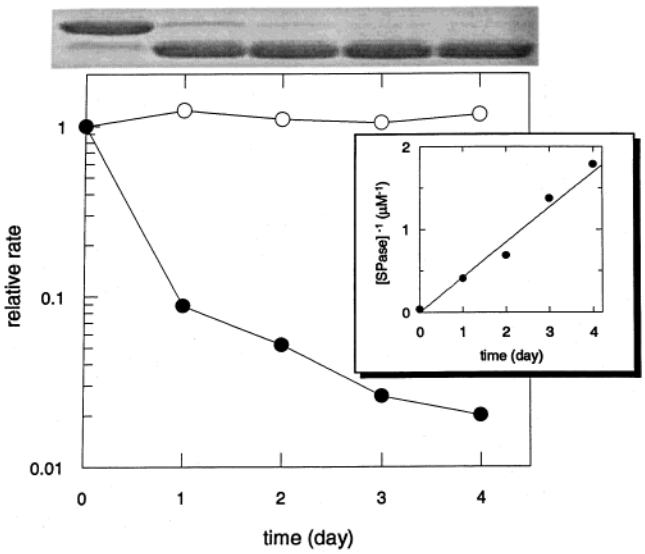

FIGURE 8: Autolysis of signal peptidase. Main plot: Signal peptidase was allowed to incubate at room temperature and, at the indicated times, assayed for hydrolytic activity toward Y^{NO2}FSASALA∼KIK^{Abz}-NH_2 (open circles) and K_5-L_{10}-Y^{NO2}FSASALA∼KIK^{Abz}-NH_2 (closed circles). Inset: Linear dependence of reciprocal SPase concentration on time has a slope of 0.42 ± 0.02 mM·day (k = 5 M^{-1} s^{-1}). Gel analysis: SDS PAGE analysis of incubation mixtures. Reaction conditions: [SPase] = 28 μM; 50 mM Tris/HCl, 1% Triton X-100, pH 8.1, RT.

steady-state kinetic parameters for SPase-catalyzed hydrolysis of this substrate are $k_c = 5 \times 10^{-3}$ s^{-1}, $K_m = 0.08$ mM, and $k_c/K_m = 63$ M^{-1} s^{-1}. The 10-fold reduction in k_c and K_m relative to FSASALA∼KI is likely due to nonproductive binding of Ac-WSASALA∼KI-AMC to SPase that is promoted by the hydrophobic character of this peptide AMC (*17*). All of these small peptide substrates incorporate structural features identified earlier as necessary for turnover by SPase: Ala at the P1 and P3 positions and a hydrophobic residue at the P7 position (*7*).

The kinetic situation is quite different for the SPase-catalyzed hydrolysis of preproteins. The most accurate kinetics have been determined for the construct proOmpA-nuclease, which is a hybrid secretory precursor of staphylococcal nuclease A fused to the signal peptide of OmpA. For the SPase-catalyzed hydrolysis of this protein $k_c = 40$ s^{-1}, $K_m = 0.02$ mM, and $k_c/K_m = 2 \times 10^6$ M^{-1} s^{-1} (*11*, *18*).

A number of published observations led us to believe that the origin of this enormous disparity in catalytic efficiency between peptide and preprotein substrates might lie in catalytically essential interactions between the signal peptide sequence of the preprotein and the transmembrane domain of SPase. First, there is the general observation that natural substrates for SPase are similar only in their signal peptide regions (*7*). Thus, determinants of substrate specificity are likely to be found here and not in the "body" of the mature protein. Second, Δ2−75 SPase, which lacks both transmembrane domains, experiences a 96% reduction in its ability to hydrolyze proOmpA-nuclease (*18*). Related to this is the observation that SPase autolyzes to a truncated species (Δ1−40 SPase) which lacks one of the two hydrophobic transmembrane domains (i.e., H1) and is unable to process preprotein substrates (*19*, *20*). Third, the signal peptide of M13 procoat is an inhibitor of the processing of both procoat and preMBP with an IC_{50} of around 2 μM (*21*).

Given these observations, we reasoned that if we appended a signal peptide-like sequence onto the N-terminus of a peptide substrate, we might be able to recover at least some portion of the catalytic efficiency of SPase as expressed toward preprotein substrates. The signal peptide mimic that we designed is K_5-L_{10}-.[2] This is based on the observations of (1) Jones and Gierasch (*22*) that K_5- can adequately serve as the positively charge N-terminus in model signal peptides and (2) Jain et al. (*23*) that -L_{10}- can serve as the hydrophobic core of model signal peptides. The Zhong and Benkovic peptide was chosen as the fluorogenic cleavage domain of our substrate (*12*).

When we combined these design elements, the resultant peptide, K_5-L_{10}-Y^{NO2}FSASALA∼KIK^{Abz}-NH_2, was observed to be efficiently hydrolyzed by SPase. Under conditions of 1% Triton X-100, which allows comparison to literature kinetic parameters (*18*), k_c/K_m for the SPase-catalyzed hydrolysis of K_5-L_{10}-Y^{NO2}FSASALA∼KIK^{Abz}-NH_2 is at least 10^4 times larger than k_c/K_m for hydrolysis of Y^{NO2}-FSASALA∼KIK^{Abz}-NH_2[3] and closely approximates the catalytic efficiency of SPase toward preprotein substrates.[4] These results support our hypothesis that the origin of the disparity in hydrolysis rates of preproteins and minimal peptide substrates (e.g., Y^{NO2}FSASALA∼KIK^{Abz}-NH_2) resides primarily in the signal peptide sequence of the preprotein. Of secondary importance are structural features of the mature protein that is being produced in the processing event. This is further supported by our finding that the C-terminal truncation of K_5-L_{10}-Y^{NO2}FSASALA∼KIK^{Abz}-NH_2 to K_5-L_{10}-Y^{NO2}FSASALA∼K^{Abz}-NH_2 is accompanied by no change in reactivity toward SPase (k_c/K_m = 450 000 M^{-1} s^{-1}; unpublished data). It is only when the leaving group completely loses peptide structural character with K_5-L_{10}-YFSASALA∼AMC that a loss of activity is observed (k_c/K_m = 16 M^{-1} s^{-1}; see below).

The actual role that is played by the signal sequence during reactions of SPase is of course a matter of some importance and will be discussed below.

Dependence of Signal Peptidase Kinetics on Micelle Concentration. In the course of our investigations of the SPase-catalyzed hydrolysis of K_5-L_{10}-Y^{NO2}FSASALA∼KIK^{Abz}-NH_2, we noted a strong dependence of catalytic activity on the concentration of Triton X-100. This is illustrated in Figure 5 where we observe inhibition of SPase activity by Triton X-100 above its CMC. Our starting point for the interpretation of these data is the concept of surface dilution kinetics developed by Dennis some 25 years ago to treat the apparently anomalous kinetics of phospholipase A2-catalyzed hydrolysis of phospholipids in Triton X-100 mixed micelles (for a recent review, see ref *24*).

Scheme 1 describes the key concepts of surface dilution kinetics (*24*) as applied to phospholipase A2 and other soluble enzymes that must associate with substrate aggregates. In a step that occurs in bulk solution, soluble enzyme, E, first combines with substrate-containing micelle, M, to form the micelle-associated enzyme species, E*. Subsequent reaction steps occur at the surface of the micelle and involve binding of substrate to the enzyme active site followed by turnover of the Michaelis complex, (E:S)*, to form micelle-associated enzyme and product. According to this mechanism, $K_{ass.}$ has units of molarity while K_s* is unitless, since it occurs on the micelle surface (*24*).

Scheme 1. Surface Dilution Kinetics

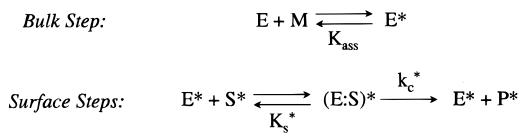

Kinetically, this reaction can be formally treated as an ordered enzyme reaction to generate the rate expression

$$v = \frac{V_{max}\hat{S}}{K_s^*\left(1 + \frac{K_{ass.}}{[TX] + [S]}\right) + \hat{S}} \quad (2)$$

where TX is Triton X-100 and $\hat{S}$ is the mole fraction of substrate in the mixed micelle, defined as:

$$\hat{S} = \frac{[S]}{[TX] + [S]} \quad (3)$$

An important feature of this mechanism is the simplification of eq 2 that occurs if we restrict ourselves to molar concentrations of substrate that are much less than the concentration of Triton X-100; that is, [S] ≪ [TX]. This condition leads to the expression

$$v = \frac{V_{max}[S]}{K_{ass.}K_s^*\left(1 + \frac{[TX]}{K_{ass.}}\right) + [S]} \quad (4)$$

or

$$v = \frac{V_{max}[S]}{K_m^*\left(1 + \frac{[TX]_{micelle}}{K_{i,M}}\right) + [S]} \quad (5)$$

where K_m* equals the product $K_{ass.}K_s$*, $[TX]_{micelle}$ is the molar concentration of Triton X-100 micelles, and $K_{i,M}$ is an inhibition constant that equals the dissociation constant for the complex formed between enzyme and a micelle that lacks substrate.

[2] A Lys-rich N-terminal region (i.e., K_5-) is not necessary for kinetic studies conducted with SPase in surfactant micelles. The substrate Ac-L_{10}-Y^{NO2}FSASALA∼KIK^{Abz}-NH_2 was prepared and has a k_c/K_m value of 180 000 M^{-1} s^{-1} (50 mM Tris/HCl, pH 8.1, 1% Triton X-100; data not shown). The N-terminal K_5- moiety was included in our substrate design strategy in anticipation of studies that we are now conducting in phospholipid vesicles where a Lys-rich N-terminal is needed (*22*, *23*). Nonetheless, in the studies reported herein, substrates with an N-terminal K_5- are still preferred over an N-terminal Ac- due to better solubility properties of the former in aqueous buffer.

[3] k_c/K_m is 2.5 × 10^5 M^{-1} s^{-1} for the SPase-catalyzed hydrolysis of K_5-L_{10}-Y^{NO2}FSASALA∼KIK^{Abz}-NH_2 (50 mM Tris/HCl, pH 8.1, 37 °C, 1% Triton X-100). Note that the value of k_c/K_m that is given for this substrate in Table 1 is 10-times larger and was determined at 0.03% Triton X-100.

[4] There is a factor 10 difference in k_c/K_m between the K_5-L_{10}-Y^{NO2}-FSASALA∼KIK^{Abz}-NH_2 and preprotein substrates. However, we believe that this difference is not mechanistically significant and is probably due to the combined effect of differences in sequence at the cleavage site as well as in the Lys-rich N-terminus and hydrophobic core of the signal peptide. The sequence of the proOmpA substrate is MKKT-AIAIAVALAGF-ATVAQA∼nuclease (Lys-rich N-terminus, hydrophobic core, and cleavage region of the signal peptide are set off by hyphens) and is substantially different from K_5-L_{10}-Y^{NO2}FSASALA ∼KIK^{Abz}-NH_2.

Scheme 2. Surface Dilution Kinetics at the Low Mole Fraction Substrate Limit

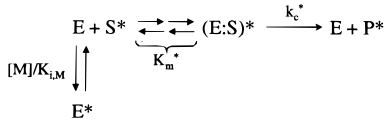

The expression of eq 5 describes the mechanism that is depicted in Scheme 2. According to this mechanism, enzyme can either combine with micelle-associated substrate to ultimately produce a Michaelis complex (E:S)* that can turnover to generate product or it can associate with a micelle that lacks substrate (i.e., an "empty" micelle) to produce an abortive or inhibitory complex. We see that in the low substrate limit, K_m* is a dissociation constant with units of molarity and reflects the energy difference between reactants, E and S*, and the complex of greatest stability that accumulates in the steady state, (E:S)*.

We can extend this model to reactions of signal peptidase as shown in Scheme 3. To explain the mechanism of this

Scheme 3. Catalysis by Signal Peptidase in Detergent Micelles[a]

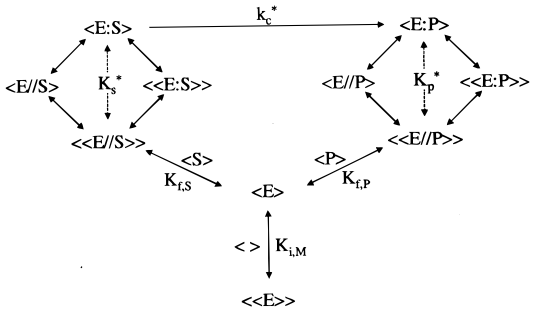

[a] In this scheme, the symbols have the following meanings: ⟨ ⟩, empty micelle; ⟨⟨ ⟩⟩, fused micelles; ⟨X⟩, micelle-bound X; ⟨E//Y⟩, detergent-separated E and Y; ⟨E:Y⟩; active site-bound Y.

model, we start with micelle-bound enzyme, ⟨E⟩, which can associate with one of three species: "empty" micelle, ⟨ ⟩; micelle-associated substrate, ⟨S⟩; micelle-associated product, ⟨P⟩. Reaction of enzyme and substrate begins with a micelle fusion (*24*, *31*, *32*, *33*) of ⟨E⟩ with ⟨S⟩ to produce the species, ⟨⟨E//S⟩⟩, in which enzyme and substrate are contained within a large, unstable aggregate but separated by surfactant molecules. This fusion event is governed by the dissociation constant $K_{f,S}$. Generation of a catalytically competent Michaelis complex, ⟨E:S⟩, is a complex event involving two separate processes: (1) diffusion of substrate through the local pool of surfactant into the enzyme active site; and (2) "shedding" of excess surfactant molecules to form a more stable micelle species (*24*, *31*, *32*, *33*) (i.e., the microscopic reverse of micelle fusion). The ordering of these two processes is unknown, but the overall process is governed by the composite term K_s* that also reflects a concerted pathway. Hydrolysis of substrate can now occur within the Michaelis complex to generate the enzyme:product complex ⟨E:P⟩.[5] Dissociation of ⟨E:P⟩ to produce free ⟨E⟩ and ⟨P⟩ is the reverse of the association of enzyme and substrate. In addition to complex formation between micelle-bound enzyme and substrate or product, ⟨E⟩ can also associate with micelles that do not contain substrate. This is an abortive event and leads to the inhibitory complex, ⟨⟨E⟩⟩.

The rate expression for the mechanism of Scheme 3 in the absence of product is given as follows:

$$v = \frac{k_c^*[E][S]}{K_{f,S}K_s^*\left(1 + \frac{[TX]_{micelle}}{K_{i,M}}\right) + [S]} \qquad (6)$$

This expression can, of course, be simplified to an expression having the form of eq 5 with the simple equality $K_m^* = K_{f,S}K_s^*$.

The mechanism of Scheme 3 and the expression of eq 6 allow us to make a number of predictions concerning the dependence of the steady-state kinetic parameters on the concentration of Triton X-100 micelles. First, the observed value of k_c/K_m should decrease with increasing $[TX]_{micelle}$ according to a simple binding isotherm and, thus, allow calculation of the inhibition constant $K_{i,M}$ and the limiting value of $(k_c/K_m)_{obs}$ or $k_c^*/(K_{f,S}K_s^*)$. Second, the observed value of the Michaelis constant should increase linearly with increasing $[TX]_{micelle}$ with *y*-intercept equal to K_m* or $K_{f,S}K_s$*. Third, the observed value of k_c should be independent of $[TX]_{micelle}$. These predictions were all realized as evidenced by the data of Figure 6 and thus support the validity of Scheme 3 as model for reactions of SPase.

Rate Limitation during Catalysis by Signal Peptidase. To probe the identity and structure of the rate-limiting transition state for SPase-catalyzed reactions, we performed solvent isotope effect measurements[6] (*25*) with two substrates of widely different reactivities toward SPase: K_5-L_{10}-Y^{NO2}-FSASALA∼KIK^{Abz}-NH_2 and K_5-L_{10}-YFSASALA∼AMC. For the SPase-catalyzed hydrolysis of K_5-L_{10}-YFSASALA∼AMC, solvent isotope effects are large and normal for both $k_{c,obs}$ and $(k_c/K_m)_{obs}$, equal to 2.2 and 2.5, respectively. These results suggest rate limitation of both process by a chemical step that is subject to protolytic catalysis. These isotope effects are consistent with the rapid-equilibrium mechanism of Scheme 3. In this mechanism, the stable complex that accumulates in the steady-state is either ⟨⟨E//S⟩⟩ or ⟨E:S⟩ and, thus, $k_{c,obs}$ and $(k_c/K_m)_{obs}$ are rate-limited k_c*. By analogy to the action of serine proteases on peptide−AMC substrates (*25*), k_c* reflects acylation of the active serine by substrate with general acid−base catalysis.

In support of this interpretation are the proton inventories of $k_{c,obs}$ and $(k_c/K_m)_{obs}$ (Figure 7). Proton inventories are experiments in which rate measurements are conducted in mixed isotopic waters and the resultant data expressed graphically as the dependence of reaction velocity, or rate constant, on mole fraction solvent deuterium (*25*). The shape of these curves reflects the number of ground state and transition state protonic sites that generate the isotope effect.

[5] In the case of substrate K_5-L_{10}-Y^{NO2}FSASALA∼KIK^{Abz}-NH_2, the product, P, is K_5-L_{10}-Y^{NO2}FSASALA. For simplicity, the other product, KIK^{Abz}-NH_2, is not shown in the mechanism of Scheme 3. This product does not associate with micelles nor does it inhibit the enzyme.

[6] While D_2O can influence the CMC, aggregation number, and structure of the micelles of certain surfactants (*26*−*28*), these changes are not significant enough to influence the interpretation of the solvent isotope effect data of this paper.

Scheme 4. Mechanism of Acylation of Ser^{90} of SPase

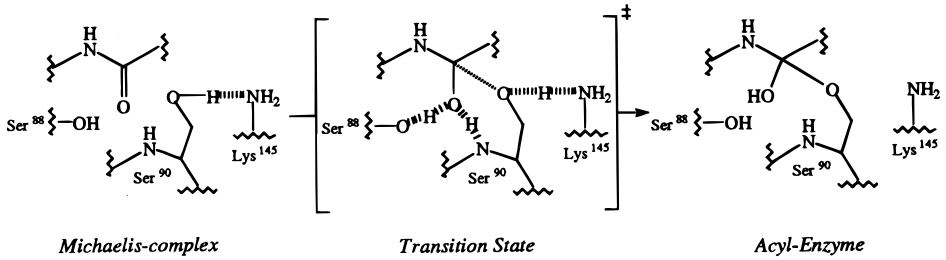

The starting point for the analysis of proton inventory data is the Gross−Butler equation shown as follows:

$$k_n = k_0 \frac{\prod(1 - n + n\phi_i^{T})}{\prod(1 - n + n\phi_j^{G})} \quad (7)$$

Here k_n is the rate constant at mole fraction solvent deuterium n, k_0 is the rate constant in pure H_2O (i.e., $n = 0$), and ϕ_i^T and ϕ_j^G are the isotopic fraction factors for the i^{th} and j^{th} proton that is transferred in the transition state and ground state, respectively. For reactions of serine proteases, ground-state fractionation factors are unity and the Gross−Butler equation simplifies to

$$k_n = k_0 \prod (1 - n + n\phi_i^{T}) \quad (8)$$

The observation of linear proton inventories for $k_{c,obs}$ and $(k_c/K_m)_{obs}$ suggests that a single protonic site generates the isotope effect and allows further simplification to:

$$k_n = k_0(1 - n + n\phi^{T}) \quad (9)$$

Fitting the data sets of Figure 7 to eq 9 generates transition state fractionation factors of $\phi^T = 0.45$ and $\phi^T = 0.40$ for $k_{c,obs}$ and $(k_c/K_m)_{obs}$, respectively.

The protonic site that generates the isotope effect is likely the proton bridge that forms between the ϵ-amine of Lys^{145} and the hydroxyl of Ser^{90} in the rate-limiting transition state for acylation of Ser^{90} by K_5-L_{10}-YFSASALA∼AMC. This is depicted in Scheme 4, where we combine results from the recent X-ray crystallization study of SPase (*8*) with our proton inventory results. Note that the hydrogen bonds from the backbone −NH of Ser^{90} and Oγ−OH of Ser^{88} that comprise the transition state-stabilizing "oxyanion hole" apparently do not contribute to the observed isotope effect as evidenced by the simple, linear proton inventory that we observe.

In contrast to the large solvent isotope effects that we observe for the SPase-catalyzed hydrolysis of K_5-L_{10}-YFSASALA∼AMC, we observe an isotope effect of unity on $(k_c/K_m)_{obs}$ for hydrolysis of K_5-L_{10}-Y^{NO2}FSASALA∼KIK^{Abz}-NH_2. This suggests a change in rate limitation from a chemical step, for hydrolysis of K_5-L_{10}-YFSASALA∼AMC, to some physical, isotopically silent step for hydrolysis of K_5-L_{10}-Y^{NO2}FSASALA∼KIK^{Abz}-NH_2. This suggests that for the SPase-catalyzed hydrolysis of K_5-L_{10}-Y^{NO2}FSASALA∼KIK^{Abz}-NH_2, turnover of the Michaelis complex to product is much faster than its reversion back to free enzyme and substrate. In this situation, a number of possibilities exist for the identity of the rate-limiting step, including (i) a conformational change of the enzyme, (ii) fusion of ⟨E⟩ with ⟨S⟩ to form ⟨⟨E//S⟩⟩ or (iii) formation of ⟨E:S⟩ from ⟨⟨E//S⟩⟩.

Origin of Rate Enhancement Observed with Signal Peptide-Based Substrates. We now return to our observation that the SPase-catalyzed hydrolysis of K_5-L_{10}-Y^{NO2}FSASALA∼KIK^{Abz}-NH_2 is several orders of magnitude faster than the hydrolysis of Y^{NO2}FSASALA∼KIK^{Abz}-NH_2. We propose that this rate enhancement originates from an "anchoring" of substrate to micelle which allows micelle-bound enzyme to have access to substrate and sets the stage for the more important development of specific interactions between the signal peptide sequence and the hydrophobic, transmembrane domains of SPase. Catalytically important interactions between SPase and the signal peptide sequence of the substrate are supported by the following:

(1) k_c* is increased by a factor of 10^2−10^3 when Y^{NO2}FSASALA∼KIK^{Abz}-NH_2 is extended to K_5-L_{10}-Y^{NO2}-FSASALA∼KIK^{Abz}-NH_2. If the N-terminal extension acted only to anchor the peptide to the micelle, this would manifest itself as an effect on the apparent binding affinity of substrate not as an effect on maximal velocity at saturating substrate concentrations.

(2) The peptide product, K_5-L_{10}-Y^{NO2}FSASALA, and its primary amide inhibit SPase with K_i values that are similar in magnitude to K_m values for the corresponding substrate. There is no reason for ⟨P⟩ to have any inhibitory effect unless, after fusion with ⟨E⟩, product can bind to the enzyme active site.

(3) The product of SPase autolysis, Δ1−40 SPase, does not hydrolyze K_5-L_{10}-Y^{NO2}FSASALA∼KIK^{Abz}-NH_2 but does hydrolyze Y^{NO2}FSASALA∼KIK^{Abz}-NH_2. This result suggests that the signal peptide sequence of the former substrate establishes catalytically essential interactions with the first transmembrane domain H1 of SPase. Δ1−40 SPase, which cannot interact with K_5-L_{10}-Y^{NO2}FSASALA∼KIK^{Abz}-NH_2 in this way, cannot catalyze hydrolysis of this substrate.

REFERENCES

1. Driessen, A. J. M., Fekkes, P., and Van der Wolk, J. P. W. (1998) *Curr. Opin. Microbiol. 1*, 216−222.
2. Economou, A. (1998) *Mol. Microbiol. 27*, 511−518.
3. Ito, K. (1996) *Genes Cells 1*, 337−346.
4. Wickner, W., and Rice-Leonard, M. (1996) *J. Biol. Chem. 271*, 29514−29516.
5. Wickner, W., Driessen, A. J. M., and Hartl, F.-U. (1991) *Annu. Rev. Biochem. 60*, 101−124.
6. den Blaauwen, T., and Driessen, A. J. M. (1996) *Arch. Microbiol. 165*, 1−8.
7. Dalbey, R. E., Lively, M. O., Bron, S., and Van Dijl, J. M. (1997) *Protein Sci. 6*, 1129−1138.

8. Paetzel, M., Dalbey, R. E., and Stryndka, N. C. J. (1998) *Nature 398*, 186−190.
9. van Klombenburg, W., Paetzel, M., de Jong, J. M., Dalbey, R. E., Demel, R. A., von Heijne, G., and de Kruijff, D. (1998) *FEBS Lett. 431*, 75−79.
10. Paetzl, M., and Dolbey, R. E. (1997) *Trends Biochem. Sci. 22*, 28−31.
11. Chatterjee, S., Suciu, D., Dalbey, R. E., Kahn, P. C., and Inouye, M. (1995) *J. Miol. Biol. 245*, 311−314.
12. Zhong, W., and Benkovic, S. J. (1998) *Anal. Biochem. 255*, 66−73.
13. Date, T., and Wickner, W. (1981) *Proc. Natl. Acad. Sci. 78*, 6106−6610.
14. March, P. E., and Inouye, M. (1985) *J. Biol. Chem. 260*, 7206−7213.
15. Devereux, J., Haeberli, M., and Smitheis, O. (1984) *Nucleic Acids Res. 12*, 387−395.
16. Dev, I. K., Ray, P. H., and Novak, P. (1990) *J. Biol. Chem. 265*, 20069−20072.
17. Kuo, D., Weidner, J., Griffin, P., Shah, S. K., and Knight, W. B. (1994) *Biochemistry 33*, 8347−8354.
18. Tschantz, W. R., Paetzl, M., Cao, G., Suciu, D., Inouye, M., and Dalbey, R. E. (1995) *Biochemistry 34*, 3935−3941.
19. Talarico, T., Dev, I. K., Bassford, P. J., and Ray, P. H. (1991) *Bichem. Biophys. Res. Commun. 181*, 650−656.
20. Ohno-Iwashita, Y., Wolfe, P., Ito, K., and Wickner, W. (1984) *Biochemistry 23*, 6178−6184.
21. Wickner, W., Moore, K., Dibb, N., Geisset, D., and Rice, M. (1987) *J. Bacteriol. 169*, 3821−3822.
22. Jones, J. D., and Gierasch, L. M. (1994) *Biophys. J. 67*, 1534−1545.
23. Jain, R. G., Rusch, S. L., and Kendall, D. A. (1994) *J. Biol. Chem. 269*, 16305−16310.
24. Carman, G. M., Deems, R. A., and Dennis, E. A. (1995) *J. Biol. Chem. 270*, 18711−18714.
25. Quinn, D. M., and Sutton, L. D. (1991) in *Enzyme Mechanism from Isotope Effects* (Cook, P. F., Ed.) CRC Press, Boston, MA, 73−126.
26. Chang, N. J., and Kaler, E. W. (1985) *J. Phys. Chem. 89*, 2996−3000.
27. Pandit, N. K., and Caronia, J. (1988) *J. Colloid Interface Sci. 122*, 100−103.
28. Mukerjee, P., Kapauan, P., and Meyer, H. G. (1966) *J. Chem. Phys. 70*, 783−786.
29. Kano, K., Ueno, Y., and Hashimoto, S. (1985) *J. Phys. Chem. 89*, 3161−3166.
30. Robson, R. J., and Dennis, E. A. (1977) *J. Phys. Chem. 81*, 1075−1078.
31. Brown, J. M. (1979) *Colloid Sci. 3*, 253−293.
32. Waton, G. (1997) *J. Phys. Chem. 101*, 9727−9731.
33. Egelhaaf, S. U. (1998) *Curr. Opin. Colloid Interface Sci. 3*, 608−613.

BI000352I